



Two-body repulsive bound pairs in a multibody interacting Bose-Hubbard model

Suman Mondal ¹, Augustine Kshetrimayum ², and Tapan Mishra¹

¹*Department of Physics, Indian Institute of Technology, Guwahati, Assam - 781039, India*

²*Dahlem Center for Complex Quantum Systems, Physics Department, Freie Universität Berlin, 14195 Berlin, Germany*



(Received 9 March 2020; revised 15 July 2020; accepted 20 July 2020; published 13 August 2020)

We study the system of multibody interacting bosons on a two-dimensional optical lattice and analyze the formation of bound bosonic pairs in the context of the Bose-Hubbard model. Assuming a repulsive two-body interaction we obtain the signatures of pair formation in the regions between the Mott insulator lobes of the phase diagram for different choices of higher-order local interactions. Considering the most general Bose-Hubbard model involving local multibody interactions we investigate the ground state properties utilizing the cluster mean-field theory approach and further confirm the results by means of sophisticated infinite projected entangled pair states calculations. By using various order parameters, we show that the choice of higher-order interaction can lead to pair superfluid phase in the system between two different Mott lobes. We also analyze the effect of temperature and density-dependent tunneling to establish the stability of the PSF phase.

DOI: [10.1103/PhysRevA.102.023312](https://doi.org/10.1103/PhysRevA.102.023312)

I. INTRODUCTION

The seminal observation of quantum phase transition between the superfluid (SF) and the Mott insulator (MI) phases in optical lattice [1] and its theoretical prediction [2,3] have revolutionized the field of strongly correlated quantum matter. The physics which emerges out of the competition between the local two-body interactions and the off-site hopping strengths of the paradigmatic Bose-Hubbard (BH) model is regarded as one of the simplest examples of quantum simulations. The underlying mechanism which drives this interesting phase transition is the high level of tunability of on-site interactions with respect to the hopping amplitudes using the technique of the Feshbach resonance and/or the lattice strengths. Following this experimental observation, several interesting phenomena have been unveiled at the interface of atomic, molecular, optical, and condensed matter physics in recent years considering many variants of the BH model. However, the simple BH model with only on-site interactions itself have revealed a plethora of exotic physics in different contexts [4–6].

Recently, effective higher-order interactions have been observed in optical lattice experiments [7,8]. These effective interactions are due to the virtual population of occupation dependent higher Bloch bands. Although these effects are small compared to the original two-body interactions, they provide enough motivation to explore the physics of ultracold matter in the presence of multibody interactions in optical lattices. An immediate usefulness of such multibody interactions can be understood in the context of the attractive BH model which involves local two-body attractive interactions. It has been shown that for any finite attractive interaction the bosons occupy a single site of an optical lattice leading to collapse [9]. This difficulty can be overcome by including a very strong three-body on-site repulsion which prevents

the occupation of a lattice site by more than two atoms and hence the collapse. A recent proposal rigorously shows that an infinitely strong three-body repulsion can arise due to the three-body loss process resulting from the elastic scattering of atoms [10]. This infinite three-body repulsion which is termed as the three-body hardcore constraint, facilitates the formation of attractively bound bosonic pairs. The superfluid of these composite pairs is called the pair superfluid (PSF) phase in optical lattice [10–13] which is an interesting manifestation of competing two- and three-body interactions. Several other theoretical proposals have been made recently to control the three-body interactions in various ways in optical lattices [14–16]. Moreover, a recent proposal by Petrov [17] reveals the possibilities to simultaneously manipulate the higher-order multibody interactions along with the two-body one in atomic systems [17,18]. This prediction is one step forward in the directions of exploring physics arising due to the on-site interactions in optical lattices. With these types of interactions, the standard BH model gets modified accordingly and one gets a more general BH model with the on-site multibody interactions given as

$$H = -t \sum_{\langle i,j \rangle} (a_i^\dagger a_j + \text{H.c.}) + \sum_{p=2}^M \left(U_p \sum_i \frac{(n_i)!}{p!(n_i-p)!} \right) - \mu \sum_i n_i, \quad (1)$$

where a_i^\dagger (a_i) is the bosonic creation (annihilation) operator, n_i is the number operator for the i th site, and $\langle i, j \rangle$ denotes the nearest-neighbor sites. While t represents the nearest-neighbor hopping amplitude, U_p is the on-site p -body interaction strength. Depending on the value of M , one gets the corresponding multibody interacting BH model. μ is the

chemical potential associated with the system in the grand canonical ensemble which decides the number of particles in the system. As mentioned before, this model with only two-body interaction U_2 exhibits the SF-MI phase transition at integer densities. As a result one gets the well-known MI lobes corresponding to different atom densities in the ground state phase diagram plotted in the μ and U_2 plane. Hereafter, we denote the MI lobes for different particle densities as MI(ρ) where ρ is the ratio between the total number of particles to total number of sites in the systems.

Although competing multibody interactions in the BH model may provide interesting physics, the system with up to the three-body interactions (U_3) has been widely studied in recent years [10,11,16,19–26] revealing various interesting physical phenomena in optical lattices. However, in an interesting proposal in Ref. [16], it is shown that the strength of the three-body interaction U_3 can be tuned by coupling it to the Efimov states which leads to a nontrivial form of the interaction $U_3\delta_{n,3}$. The phase diagram of the BH model in the presence of such three-body interaction is obtained by using the simple mean-field theory approach analysis and complemented by the quantum Monte Carlo (QMC) calculation. This reveals that for attractive U_3 and repulsive U_2 the system favors a direct first-order transition from the MI(1) to the MI(3) phase by completely suppressing the MI(1) lobe when $|U_3/U_2| > 1$ even at finite temperature [16]. However, this finding was later found to be inconsistent when compared to the density matrix renormalization group (DMRG) and the cluster mean-field theory (CMFT) calculations in one- and two-dimensional systems, respectively, by some of us in Ref. [27]. A careful analysis in Ref. [27] showed that there exists no first-order transition between the Mott lobes for the parameter choice considered in Ref. [16]. Rather, the competing two- and three-body interactions lead to the formation of a nontrivial PSF phase in between the MI(1) and MI(3) lobes where the bosons tend to move in pairs even in the presence of the two-body repulsive interactions. This reveals a kind of two-body repulsively bound pairs driven by a mechanism completely different from the one observed in optical lattices by Winkler *et al.* [28] where the pair formation occurs due to the competition between the two-body interaction U_2 and the bandwidth.

In this paper we show that to achieve this anomalous pairing of bosons with two-body repulsion, it is not always necessary to consider the specific form of the three-body interaction as discussed in Refs. [16,27]. The most general BH model given in Eq. (1) with a suitable choice of multibody interactions may stabilize the PSF phase between the Mott lobes which will be discussed in more detail below. The remaining part of the paper is organized as follows. In Sec. II we explain the model considered for this work with a brief information about the methods. In Sec. III we discuss our results in detail and finally we conclude in Sec. IV.

II. METHOD

We numerically investigate the model shown in Eq. (1) by restricting up to four-body interactions for simplicity. The explicit form of the Hamiltonian with all the interactions is

given as

$$\begin{aligned}
 H = & -t \sum_{\langle i,j \rangle} (a_i^\dagger a_j + \text{H.c.}) + \frac{U_2}{2} \sum_i n_i(n_i - 1) \\
 & + \frac{U_3}{6} \sum_i n_i(n_i - 1)(n_i - 2) \\
 & + \frac{U_4}{24} \sum_i n_i(n_i - 1)(n_i - 2)(n_i - 3) \\
 & - \mu \sum_i n_i,
 \end{aligned} \tag{2}$$

where the terms have their usual meaning as discussed before. In order to analyze the ground state properties of Eq. (2) we first utilize the self-consistent CMFT approach which is an approximation method based on the simple single site mean-field theory approach [29–31]. In this case, the Hamiltonian is divided into several clusters of finite number of sites and each cluster interacts with the rest of the system in a mean-field way, i.e.,

$$H_{\text{CMF}} = \sum_{i,j \in C} H_C - t \sum_{\substack{\langle i,j \rangle \\ i \in B, j \notin C}} (a_i^\dagger \psi_j + \text{H.c.}). \tag{3}$$

Here H_C is the cluster Hamiltonian identical to Eq. (2) with index i, j belonging to the cluster C . The second term which is the mean-field expression for the hopping term from the i th site at the cluster boundaries (B) to the nearest neighbor [32]. ψ is the superfluid order parameter which is determined self-consistently. In order to obtain the insights about various quantum phases, we utilize the average density and the superfluid density of the system $\rho = 1/L \sum_i n_i$ and $\rho_s = 1/L \sum_i \psi_i^2$, respectively, computed from the CMFT ground state where L is number of sites in a cluster. It is well known that the CMFT method is more accurate than the simple mean-field theory approach and can capture the qualitative picture of the system with less computing effort than the powerful QMC method [12,27,29–31,33]. Note that the accuracy of the method relies on the cluster size. In this case we consider a four-site cluster which is sufficient to predict the relevant physics.

In addition to the CMFT approach, we have employed the infinite projected entangled pair states (iPEPS) algorithm which are two-dimensional tensor network techniques [34,35]. Such techniques are built upon genuine quantum correlations and hence goes beyond mean-field calculations. Besides, we can directly target the thermodynamic limit by assuming translational invariance over some sites. Another advantage is that unlike QMC techniques, it does not suffer from the infamous sign problem for fermionic and frustrated systems [36]. For these reasons PEPS techniques have been used in the past to study hard condensed matter problems such as frustrated kagome antiferromagnets [37–40] and real materials [41,42]. It has been able to beat state-of-the-art QMC calculations in finding the ground state energy of the doped Hubbard model [43], and helped settle controversies that would have otherwise been difficult such as the magnetization plateaus of the Shastry-Sutherland model [44], phase diagrams of steady

states of dissipative spin models [45], etc. The technique has now been extended to finite temperature calculations [46–49] and the difficult problem of time evolution in two dimensions [50–53].

For the purpose of this work, we use an iPEPS with a two-site unit cell in the thermodynamic limit. We approximate the ground state of the Hamiltonian given in Eq. (2) using the so-called simple update [54] with bond dimension $D = 2$ and $D = 4$ which proves sufficient for our purpose. In Sec. III we provide the plots for $D = 4$. After analyzing the zero temperature phase diagram of the system we investigate the effect of thermal fluctuation in the system. The finite temperature calculations are done with an annealing algorithm [49] with infinite projected entangled pair operators (iPEPOs) which are mixed state version of iPEPS [45,55]. The expectation values are computed using the corner transfer matrix renormalization (CTMRG) method [56,57].

III. RESULTS AND DISCUSSION

In this section we move on to discuss our results in detail which are obtained by using the CMFT and iPEPS approach for $M = 4$ of Eq. (1). Keeping terms up to $M = 4$ in the model (1) we have three different interactions in the system such as U_2 , U_3 , and U_4 . Note that in our analysis the focus is to analyze the two-body repulsive bound pairs. Therefore, our obvious choice is to keep $U_2 > 0$. In this case we consider attractive (repulsive) three- (four-)body interactions, i.e., $U_3 < 0$ and $U_4 > 0$. For simplicity we define two ratios such as U_4/U_3 and U_3/U_2 and analyze the ground state phase diagram of the system. In the case of the BH model shown in Eq. (1), it is well known that the presence of interaction up to U_3 largely affects the SF-MI phase transitions with modified Mott lobes at higher densities. While the MI lobes corresponding to $\rho \geq 2$ get enlarged by the three-body repulsion U_3 [19,21], an attractive U_3 results in shrinking up of the higher MI lobes [21]. However, in this case we show that a large four-body repulsive interaction U_4 leads to interesting phenomena. Note that the large U_4 is necessary to prevent the collapse due to attractive U_3 and also to stabilize the MI(3) state in the system. In this case, the MI(3) lobe expands by simultaneously shrinking the MI(2) lobe which eventually disappears for some specific ratio of interactions defined above. In Fig. 1 we depict the phase diagram corresponding to the ground state of Eq. (3) using the CMFT approach in the μ/U_2 and $1/U_2$ plane for $U_4/U_3 = -3$ and $U_3/U_2 = -2$. The MI lobes are denoted by the continuous lines and the dashed line separates the empty state. The SF to MI transitions are characterized by examining the behavior of change in the total density of the system ρ and the superfluid density ρ_s with respect to increase in chemical potential μ . In the SF phase ρ increases continuously with an increase in μ . However, in the MI phase ρ remains constant for a range of μ and at the same time ρ_s vanishes. In Fig. 2(a) we show the $\rho - \frac{\mu}{U_2}$ plot determined using the CMFT approach for various values of $1/U_2 = 0.02$, 0.04, and 0.06 which cut through different regions of the phase diagram of Fig. 1 indicating the MI plateaus and the SF regions. The end points of the plateaus correspond to two different chemical potentials μ^+ and μ^- of the system defined

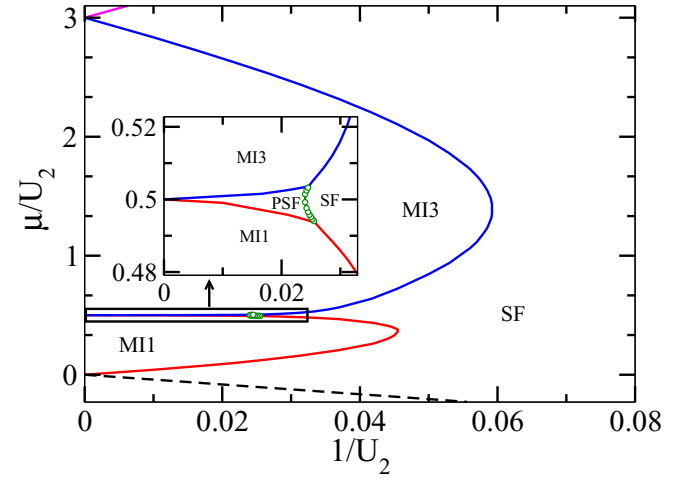


FIG. 1. CMFT phase diagram for $t = 1$, $U_3/U_2 = -2.0$, and $U_4/U_3 = -3.0$. Solid lines show the boundaries of MI phases and the dashed line separates the empty state. The inset shows the PSF-SF boundary marked by the green line with circles.

as

$$\mu^+ = E_L(N+1) - E_L(N); \quad \mu^- = E_L(N) - E_L(N-1). \quad (4)$$

Here $E(N)$ denotes the ground state energy of the system with N particles. The difference $G = \mu^+ - \mu^-$ quantifies the gap in the MI phase which vanishes in the SF phase. The signatures of the MI and SF phases are also confirmed from the $\frac{\mu}{U_2} - \rho_s$ plot in Fig. 2(b) which shows finite (zero) superfluid density in the SF (MI) phase.

Interesting thing happens in the regime of large interactions. It can be seen from Fig. 3 that for large $U_2 = 50$ ($1/U_2 = 0.02$), there are discrete jumps $\Delta\rho = 0.5$ in ρ (blue down triangles) with respect to increase in $\frac{\mu}{U_2}$ in the region

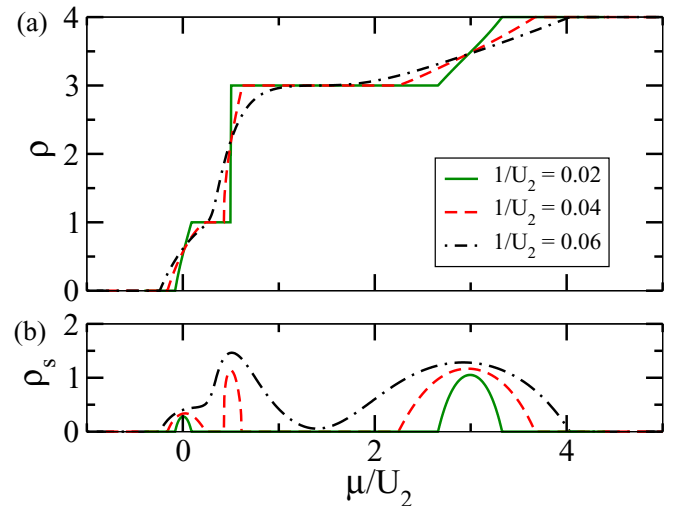


FIG. 2. (a) ρ vs μ/U_2 and (b) ρ_s vs μ/U_2 plots for several cuts through the phase diagram of Fig. 1 corresponding to 0.02 (green solid line), 0.04 (red dashed line), and $1/U_2 = 0.06$ (black dot-dashed line).

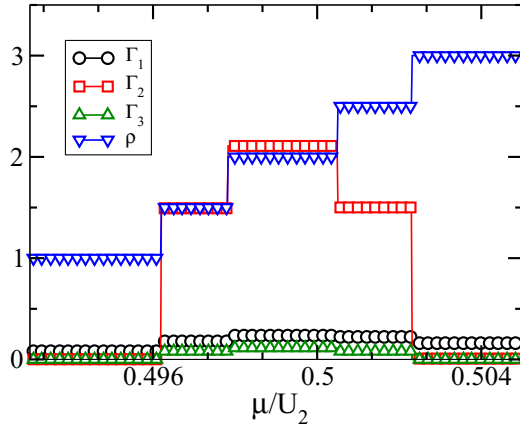


FIG. 3. Correlation functions $\Gamma_n(i, j)$ for a cut along $1/U_2 = 0.02$ in the phase diagram Fig. 1. The corresponding values of ρ (blue down triangles) are shown for comparison.

between two plateaus corresponding to the MI(1) and MI(3) phases. This indicates a change in the particle number $\Delta N = 2$, since we have $L = 4$ in our CMFT calculation, in the region which is a signature of pair formation. We can identify this phase as the PSF phase which can be confirmed from the pair correlation functions [12,27,58]. To this end we compute the n -particle nearest-neighbor correlation functions using the CMFT approach defined as

$$\Gamma_n = \langle (a_i^\dagger)^n (a_j)^n \rangle, \quad (5)$$

where i and j are the nearest-neighbor site index of our four-site cluster.

In Fig. 3 we also plot the correlation functions Γ_n for $n = 1, 2$, and 3 corresponding to the single- (black circles), two- (red squares), and three-particles (green up triangles), respectively, for different values of μ/U_2 at a fixed $1/U_2 = 0.02$ of the phase diagram given in Fig. 1. It can be seen that at the plateau regions corresponding to the MI(1) and MI(3) phases, all the correlation functions are vanishingly small. However, for the values of ρ away from the plateau regions, i.e., $1 < \rho < 3$, Γ_2 clearly dominates over Γ_1 and Γ_3 . This is a clear indication of the existence of the PSF phase which is sandwiched between the MI(1) and MI(3) lobes in the large U_2 regime as shown in Fig. 1. There exists a SF-PSF phase transition at these densities indicated by the green circles.

As mentioned before, the CMFT approach can predict the quantum phases qualitatively and efficiently. However, to concretely establish the existence of the PSF phase of these two-body repulsively bound pairs we use the iPEPS method discussed before. In our simulation we use various physical quantities to identify different quantum phases. The gapped MI phases are identified by looking at the behavior of the chemical potential μ with respect to the average density ρ . The SF and the PSF phases are characterized by their respective order parameters defined as

$$O_{\text{SF}} = |\langle a_i \rangle|^2 \quad (6)$$

and

$$O_{\text{PSF}} = |\langle a_i^2 \rangle|^2. \quad (7)$$

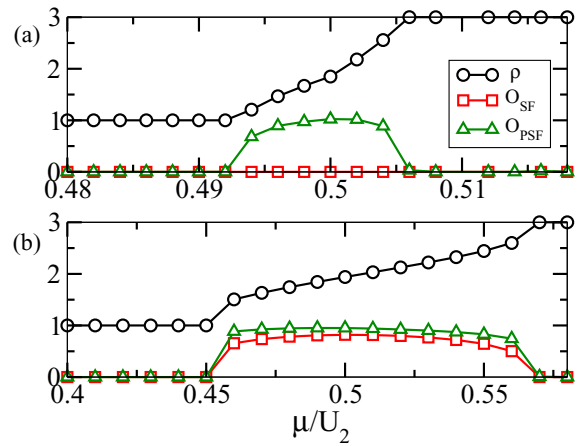


FIG. 4. (a) iPEPS data for ρ , O_{SF} , and O_{PSF} for $1/U_2 = 0.015$ showing the MI(1), MI(3), and the PSF phases. (b) Similar calculations for a cut passing through the normal superfluid (SF) region at $1/U_2 = 0.04$. This phase is characterized by a nonvanishing value of both O_{SF} as well as O_{PSF} while the PSF phase is characterized by a vanishing O_{SF} and nonzero O_{PSF} .

We compute these parameters for several values of U_2 and find signatures of different phases and phase transitions similar to that obtained using the CMFT method. In Fig. 4(a) we plot ρ (black circles), O_{SF} (red squares), and O_{PSF} (green triangles) against μ/U_2 for fixed $1/U_2 = 0.015$, $U_3/U_2 = -2$, and $U_4 = \infty$. Note that the choice of U_4 restricts the local Hilbert space to a maximum of three particles per site and simplifies our iPEPS calculation while retaining the underlying physics of the system. It can be clearly seen from Fig. 4(a) that there exists two Mott plateaus at $\rho = 1$ and 3 corresponding to the gapped MI(1) and MI(3) phases. Inside these plateau regions both superfluid order parameters vanish. However, in the region between the two MI phases, the value of O_{SF} remains vanishingly small, whereas O_{PSF} becomes finite indicating the existence of the PSF phase. We have also performed the same calculation for a different cut that passes through the region of normal superfluid (SF) as shown in Fig. 4(b) for $1/U_2 = 0.04$. We find that both the O_{SF} as well as the O_{PSF} are nonzero in this region which defines our SF phase.

It can be noted that the physics obtained using the CMFT approach and the iPEPS method are similar to the one reported in Ref. [27]. The important difference is the choice of the interactions. We explicitly show that in the presence of two-body repulsion the bosons prefer to move in pairs due to the large three-body attraction and four-body repulsion. The physics of the pair formation and the PSF phase on top of the MI(1) phase can be understood from the energy consideration as discussed in Ref. [27]. Due to the large three-body attraction the system will tend to acquire two particles at a time to reach the energy minimum by forming a trimer. However, because of the presence of uniform two-body repulsion from the MI(1) background the added particles tend to move in pairs without affecting the system energy. This leads to the PSF phase in the system. This is indeed an interesting manifestation of the multibody interactions in the Bose-Hubbard model. We would like to mention that this pair formation is not limited to the region between the MI(1) and MI(3) lobes.

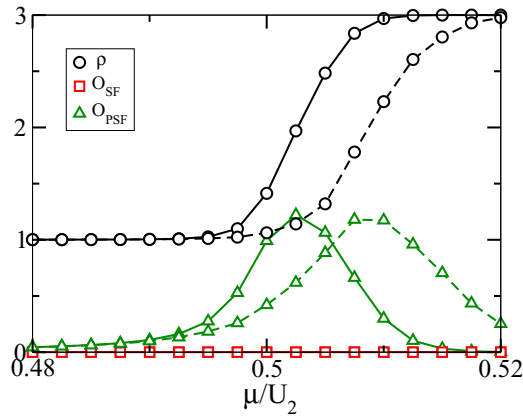


FIG. 5. iPEPS data for ρ , O_{SF} , and O_{PSF} for $1/U_2 = 0.015$ at finite temperature. Here continuous and dashed lines are corresponding to temperature $T = 0.1$ and 0.2 , respectively, where T is the inverse of the thermodynamic β .

One can in principle create the PSF phase between higher Mott lobes such as between the MI(2) and MI(4) lobes. To achieve this one needs to consider a five-body interaction term by keeping terms up to $M = 5$ in the model given in Eq. (1). Using the CMFT calculation we verify that the PSF in this case can be obtained for suitable choice of repulsive U_2, U_3, U_5 , and attractive U_4 terms in Eq. (1). Because of the attractive nature of U_4 in this case, the value of U_5 has to be very strong and repulsive to prevent the collapse.

A. Finite temperature analysis

After discussing the zero temperature phase diagram of the model shown in Eq. (2) we embark on to analyze the effect of temperature on the system. As it is well known that the temperature is an unavoidable parameter in the real cold gas experiment [11,59,60] and the quantum phases are fragile in presence of thermal fluctuation, it is pertinent to examine the stability of the PSF phase. At this stage we perform finite temperature calculations using iPEPOs to check the survival of the PSF phase by gradually increasing the system temperature T (T is the inverse of the thermodynamic β). We compute the different order parameters for these thermal states, i.e., O_{SF} and O_{PSF} along with ρ for the same choice of parameters considered in Fig. 4(a) for the zero temperature calculation and plot them in Fig. 5. We show two different values of temperature such as $T = 0.1$ and $T = 0.2$ at which the PSF phase clearly survives which can be seen from the finite values of O_{PSF} . Above this temperature the PSF phase slowly disappears. This confirms that the PSF phase is stable against the thermal fluctuation.

B. Effect of density induced tunneling

In this subsection we analyze the effect of density-induced tunneling on the PSF phase [61]. It has been theoretically shown that in optical lattice experiments, the density induced tunneling plays an important role and has been experimentally observed recently [62]. Although the amplitudes of such tunneling are small compared to the conventional tunneling amplitude t of the model shown in Eq. (2), the natural question

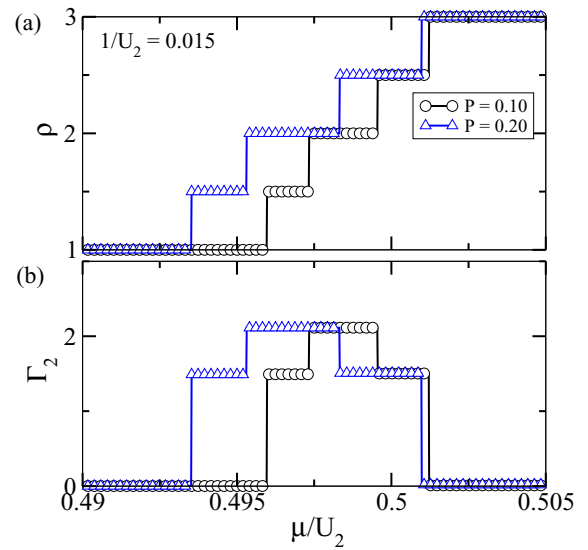


FIG. 6. The figure shows the existence of the PSF phase in the presence of density-induced tunneling (P). Here we plot particle density (ρ) in (a) and pair correlation function (Γ_2) in (b) for $P = 0.1$ (black lines with circles) and 0.2 (blue lines with triangles). The other parameters are the same as considered in Fig 1 at $U_2 = 1/0.015$.

to ask is whether the narrow region of the PSF phase will survive in the presence of such density induced tunneling or not. In this context we introduce the density-induced tunneling term in Eq. (2) which is given by

$$H_P = -P \sum_{\langle i,j \rangle} (a_i^\dagger (n_i + n_j) a_j + \text{H.c.}), \quad (8)$$

where P is the density-induced tunneling amplitude. Using the CMFT approach, we show that, indeed, the PSF phase survives up to a finite value of P . In the CMFT method, the density-dependent tunneling term can be decoupled as

$$a_i^\dagger (n_i + n_j) a_j \approx \psi (a_i^\dagger n_i + n_j a_j), \quad (9)$$

where the terms $O(\psi^3)$ are neglected [63] and ψ is the superfluid order parameter.

In Fig. 6 we plot the behavior of various physical quantities with respect to P for a cut through the phase diagram of Fig. 1 at $1/U = 0.015$ which passes through the PSF phase. It can be seen from Fig. 6(a), where we plot particle density (ρ) for $P = 0.1$ and 0.2 , that the ρ exhibits discrete jumps in steps of $\delta\rho = 0.5$, indicating a PSF phase. The corresponding pair correlation function (Γ_2) are plotted in Fig. 6(b) which confirm the existence of the PSF phase for finite values of P . However, when we further increase the P , the system exhibits a normal SF phase for $P = 0.3$. We also analyze this situation using the iPEPS method which is shown in Fig. 7. The figure depicts that the O_{PSF} (O_{SF}) is finite (zero) for finite values of P , indicating the existence of the PSF phase.

IV. CONCLUSIONS

In this paper we analyze a multibody interacting Bose-Hubbard model and show the possibility of creating two-body repulsive bound bosonic pairs in a two-dimensional optical

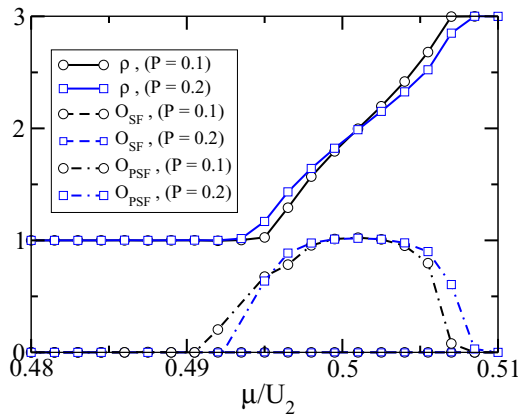


FIG. 7. The existence of PSF phase for different values of density dependent hopping amplitude P . Here we plot ρ (solid lines), O_{SF} (dashed lines), and O_{PSF} (dot-dashed lines) for $P = 0.1$ and 0.2 , which indicate that the PSF survives for finite values of P .

lattice due to the combined effects of the many-body interactions. We establish that for a very strong four-body repulsion a suitable ratio between the three-body attraction and two-body

repulsion leads to the pair formation and hence the PSF phase between the MI(1) and MI(3) lobes. This fact is concretely demonstrated by analyzing the ground state properties of the BH model using the CMFT approach as well as the iPEPS method. Moreover, we show that this pair formation is stable against the thermal fluctuation and density induced tunneling effects which are inevitable in cold gas experiments. Due to the recent development in the field of ultracold quantum gas experiments, if it can be made possible to engineer the many-body interactions among the bosons, then it will be possible to create the repulsively bound pairs in an alternate way as opposed to the already observed one [28]. Moreover, this finding may provide scope to create and manipulate the number of pairs in a controlled manner.

ACKNOWLEDGMENTS

T.M. acknowledges DST-SERB India for the financial support through Project No. ECR/2017/001069. Part of the computational simulations were carried out using the computational facilities of Param-Ishan at Indian Institute of Technology, Guwahati, India.

- [1] M. Greiner, O. Mandel, T. Esslinger, T. W. Hänsch, and I. Bloch, *Nature (London)* **415**, 39 (2002).
- [2] M. P. A. Fisher, P. B. Weichman, G. Grinstein, and D. S. Fisher, *Phys. Rev. B* **40**, 546 (1989).
- [3] D. Jaksch, C. Bruder, J. I. Cirac, C. W. Gardiner, and P. Zoller, *Phys. Rev. Lett.* **81**, 3108 (1998).
- [4] I. Bloch, J. Dalibard, and W. Zwerger, *Rev. Mod. Phys.* **80**, 885 (2008).
- [5] M. P. Kennett, *ISRN Condens. Matter Phys.* **2013**, 39 (2013).
- [6] M. Lewenstein, A. Sanpera, V. Ahufinger, B. Damski, A. Sen(De), and U. Sen, *Adv. Phys.* **56**, 243 (2007).
- [7] S. Will, T. Best, U. Schneider, L. Hackermüller, D.-S. Lühmann, and I. Bloch, *Nature (London)* **465**, 197 (2010).
- [8] M. J. Mark, E. Haller, K. Lauber, J. G. Danzl, A. J. Daley, and H.-C. Nägerl, *Phys. Rev. Lett.* **107**, 175301 (2011).
- [9] F. Dalfovo, S. Giorgini, L. P. Pitaevskii, and S. Stringari, *Rev. Mod. Phys.* **71**, 463 (1999).
- [10] A. J. Daley, J. M. Taylor, S. Diehl, M. Baranov, and P. Zoller, *Phys. Rev. Lett.* **102**, 040402 (2009).
- [11] L. Bonnes and S. Wessel, *Phys. Rev. Lett.* **106**, 185302 (2011).
- [12] M. Singh, T. Mishra, R. V. Pai, and B. P. Das, *Phys. Rev. A* **90**, 013625 (2014).
- [13] Y.-C. Chen, K.-K. Ng, and M.-F. Yang, *Phys. Rev. B* **84**, 092503 (2011).
- [14] P. R. Johnson, E. Tiesinga, J. V. Porto, and C. J. Williams, *New J. Phys.* **11**, 093022 (2009).
- [15] A. J. Daley and J. Simon, *Phys. Rev. A* **89**, 053619 (2014).
- [16] A. Safavi-Naini, J. von Stecher, B. Capogrosso-Sansone, and S. T. Rittenhouse, *Phys. Rev. Lett.* **109**, 135302 (2012).
- [17] D. S. Petrov, *Phys. Rev. A* **90**, 021601(R) (2014).
- [18] D. S. Petrov, *Phys. Rev. Lett.* **112**, 103201 (2014).
- [19] M. Singh, A. Dhar, T. Mishra, R. V. Pai, and B. P. Das, *Phys. Rev. A* **85**, 051604(R) (2012).
- [20] B.-I. Chen, X.-b. Huang, S.-p. Kou, and Y. Zhang, *Phys. Rev. A* **78**, 043603 (2008).
- [21] T. Sowiński, *Phys. Rev. A* **85**, 065601 (2012).
- [22] T. Sowiński, R. W. Chhajlany, O. Dutta, L. Tagliacozzo, and M. Lewenstein, *Phys. Rev. A* **92**, 043615 (2015).
- [23] S. Ejima, F. Lange, H. Fehske, F. Gebhard, and K. zu Münster, *Phys. Rev. A* **88**, 063625 (2013).
- [24] J. Silva-Valencia and A. Souza, *Eur. Phys. J. B* **85**, 161 (2012).
- [25] C. Avila, R. Franco, A. Souza, M. Figueira, and J. Silva-Valencia, *Phys. Lett. A* **378**, 3233 (2014).
- [26] A. F. Hincapie-F, R. Franco, and J. Silva-Valencia, *Phys. Rev. A* **94**, 033623 (2016).
- [27] M. Singh, S. Greschner, and T. Mishra, *Phys. Rev. A* **98**, 023615 (2018).
- [28] K. Winkler, G. Thalhammer, F. Lang, R. Grimm, J. Hecker Denschlag, A. J. Daley, A. Kantian, H. P. Büchler, and P. Zoller, *Nature (London)* **441**, 853 (2006).
- [29] T. McIntosh, P. Pisarski, R. J. Gooding, and E. Zaremba, *Phys. Rev. A* **86**, 013623 (2012).
- [30] D. Yamamoto, A. Masaki, and I. Danshita, *Phys. Rev. B* **86**, 054516 (2012).
- [31] S. R. Hassan and L. de' Medici, *Phys. Rev. B* **81**, 035106 (2010).
- [32] A. Tomadin, V. Giovannetti, R. Fazio, D. Gerace, I. Carusotto, H. E. Türeci, and A. Imamoglu, *Phys. Rev. A* **81**, 061801(R) (2010).
- [33] D.-S. Lühmann, *Phys. Rev. A* **87**, 043619 (2013).
- [34] J. Jordan, R. Orus, G. Vidal, F. Verstraete, and J. I. Cirac, *Phys. Rev. Lett.* **101**, 250602 (2008).
- [35] F. Verstraete and J. I. Cirac, [arXiv:cond-mat/0407066](https://arxiv.org/abs/cond-mat/0407066).
- [36] P. Corboz, R. Orús, B. Bauer, and G. Vidal, *Phys. Rev. B* **81**, 165104 (2010).
- [37] H. J. Liao, Z. Y. Xie, J. Chen, Z. Y. Liu, H. D. Xie, R. Z. Huang, B. Normand, and T. Xiang, *Phys. Rev. Lett.* **118**, 137202 (2017).

- [38] T. Picot and D. Poilblanc, *Phys. Rev. B* **91**, 064415(R) (2015).
- [39] T. Picot, M. Ziegler, R. Orús, and D. Poilblanc, *Phys. Rev. B* **93**, 060407(R) (2016).
- [40] A. Kshetrimayum, T. Picot, R. Orús, and D. Poilblanc, *Phys. Rev. B* **94**, 235146 (2016).
- [41] A. Kshetrimayum, C. Balz, B. Lake, and J. Eisert, [arXiv:1904.00028](https://arxiv.org/abs/1904.00028).
- [42] C. Boos, S. P. G. Crone, I. A. Niesen, P. Corboz, K. P. Schmidt, and F. Mila, *Phys. Rev. B* **100**, 140413(R) (2019).
- [43] P. Corboz, *Phys. Rev. B* **93**, 045116 (2016).
- [44] P. Corboz, T. M. Rice, and M. Troyer, *Phys. Rev. Lett.* **113**, 046402 (2014).
- [45] A. Kshetrimayum, H. Weimer, and R. Orus, *Nat. Commun.* **8**, 1291 (2017).
- [46] P. Czarnik, L. Cincio, and J. Dziarmaga, *Phys. Rev. B* **86**, 245101 (2012).
- [47] P. Czarnik and J. Dziarmaga, *Phys. Rev. B* **92**, 035152 (2015).
- [48] P. Czarnik, M. M. Rams, and J. Dziarmaga, *Phys. Rev. B* **94**, 235142 (2016).
- [49] A. Kshetrimayum, M. Rizzi, J. Eisert, and R. Orús, *Phys. Rev. Lett.* **122**, 070502 (2019).
- [50] C. Hubig and J. I. Cirac, *SciPost Phys.* **6**, 31 (2019).
- [51] P. Czarnik, J. Dziarmaga, and P. Corboz, *Phys. Rev. B* **99**, 035115 (2019).
- [52] A. Kshetrimayum, M. Goihl, and J. Eisert, [arXiv:1910.11359](https://arxiv.org/abs/1910.11359).
- [53] A. Kshetrimayum, M. Goihl, D. M. Kennes, and J. Eisert, [arXiv:2004.07267](https://arxiv.org/abs/2004.07267).
- [54] H. C. Jiang, Z. Y. Weng, and T. Xiang, *Phys. Rev. Lett.* **101**, 090603 (2008).
- [55] H. Weimer, A. Kshetrimayum, and R. Orús, [arXiv:1907.07079](https://arxiv.org/abs/1907.07079).
- [56] R. Orús and G. Vidal, *Phys. Rev. B* **80**, 094403 (2009).
- [57] R. Orús, *Phys. Rev. B* **85**, 205117 (2012).
- [58] M. Singh, S. Mondal, B. K. Sahoo, and T. Mishra, *Phys. Rev. A* **96**, 053604 (2017).
- [59] F. Gerbier, *Phys. Rev. Lett.* **99**, 120405 (2007).
- [60] T. K. Kopec and M. W. Szymanski, *Phys. Lett. A* **378**, 3402 (2014).
- [61] O. Dutta, M. Gajda, P. Hauke, M. Lewenstein, D.-S. Lühmann, B. A. Malomed, T. Sowiński, and J. Zakrzewski, *Rep. Prog. Phys.* **78**, 066001 (2015).
- [62] O. Jürgensen, F. Meinert, M. J. Mark, H.-C. Nägerl, and D.-S. Lühmann, *Phys. Rev. Lett.* **113**, 193003 (2014).
- [63] D.-S. Lühmann, O. Jürgensen, and K. Sengstock, *New J. Phys.* **14**, 033021 (2012).